

## **Effects of Approximations on Buckling and Postbuckling Analysis**

HAI-QING YUAN

Institute of Civil Engineering and Architecture, Wuhan University of Technology,  
Wuhan, Hubei, 430070, PRC

YONG-LIN PI\*

Department of Civil Engineering, The University of Sydney, 2006, NSW, Australia

### **ABSTRACT**

Flexural-torsional buckling and postbuckling of beams can be analysed using finite element methods. In formulating a finite beam element, a rotation matrix is used to obtain strain-displacement relationships. Because of couplings between displacements and twist rotations, components of the rotation matrix are lengthy and complicated. To facilitate the formulation, approximations are usually used to simplify the rotation matrix. A simplified small rotation matrix is often used in the buckling analysis and a simplified second order rotation matrix is used for nonlinear postbuckling analysis. However, the small rotation and second order rotation matrices do not describe rotations accurately and introduce some approximations to the couplings between displacements and rotations. These approximations may affect results of buckling and postbuckling analysis. In the inelastic buckling and postbuckling analysis, numerical integration over the cross-section is usually used to check the yield criterion and to calculate the stress resultants and elastic-plastic stress-strain matrix. An integration scheme that is not consistent with stress distributions may lead to incorrect inelastic buckling and postbuckling results.

This paper investigates effects of these approximations on buckling and postbuckling analysis of beams. It is shown that a finite element model based on the small rotation matrix predicts incorrect buckling loads. A finite element model based on the second order rotation matrix may lead to over-estimations of inelastic buckling loads and poor predictions of the postbuckling behaviour. An integration scheme over the cross-section that is not consistent with stress distributions does not predict correct inelastic buckling and postbuckling behaviour.

### **INTRODUCTION**

Flexural-torsional buckling and postbuckling of beams have been studied for decades by a number of researchers. Finite element methods can be used to analyse flexural-torsional buckling and postbuckling of beams. In formulating a finite beam element, a rotation matrix is used to obtain strain-displacement relationships. Because of couplings between displacements and twist rotations, components of the rotation matrix are lengthy and complicated. To facilitate the formulation, approximations are usually used to simplify the rotation matrix. A simplified small rotation matrix is often used for the buckling analysis by a number of researchers because the rotations are small at buckling. A simplified second order rotation matrix is used for the buckling and postbuckling analysis because the second order rotation matrix is considered to have sufficient accuracy. However, neither the small rotation nor the second order rotation matrix describes rotations accurately because some

approximations to the couplings between displacements and rotations are introduced. These approximations may affect results of buckling and postbuckling analysis as pointed by Simo and Vu-Quoc (1987) and Pi and Trahair (1994).

In the inelastic analysis, to check the yield criterion and to calculate the stress resultants and elastic-plastic stress-strain matrix, numerical integration over the cross-section is usually used. The accuracy of the integration is related not only to the integration technique, but also to the arrangement scheme of the integration points. If the scheme is not consistent with the stress distributions, very accurate integration technique may produce incorrect results.

This paper investigates the effects of approximations in the rotation matrix and in the integration scheme on the buckling and postbuckling analysis of beams.

## SOME BASIC CONCEPTS

### Basic Assumptions and Rotation Matrix

Basic assumptions are: (1) strains are small; (2) Euler-Bernoulli bending theory and Vlasov's torsion theory are used; (3) beams are of doubly symmetric I-section.

Two axis systems are used to describe the motion of a thin-walled member. The first axis system  $OXYZ$  is fixed in space as shown in Fig. 1. The second axis system  $o^*x^*y^*z^*$  is attached to the beam. Before deformation, the origin  $o$  is at the centroid of the cross-section at coordinates  $(0, 0, z)$  in the axis system  $OXYZ$ . The axis  $oz$  coincides with the axis  $OZ$  and the axes  $ox$  and  $oy$  coincide with the principal axes of the cross-section before deformation. Basis vectors of the system  $oxyz$  are  $\vec{p}_x, \vec{p}_y, \vec{p}_z$ . After deformation, the centroid  $o$  displaces  $u, v, w$  in the directions  $OX, OY, OZ$  to point  $o^*$  and at the same time the cross-section rotates through an angle  $\phi$ , so that the beam-attached axis system moves to  $o^*x^*y^*z^*$ . The axis  $o^*z^*$  is in the tangential direction of the deformed centroidal axis. The axes  $o^*x^*$  and  $o^*y^*$  coincide with the principal axes of the cross-section of the deformed member. Basis vectors of the system  $o^*x^*y^*z^*$  are  $\vec{q}_x, \vec{q}_y, \vec{q}_z$ .

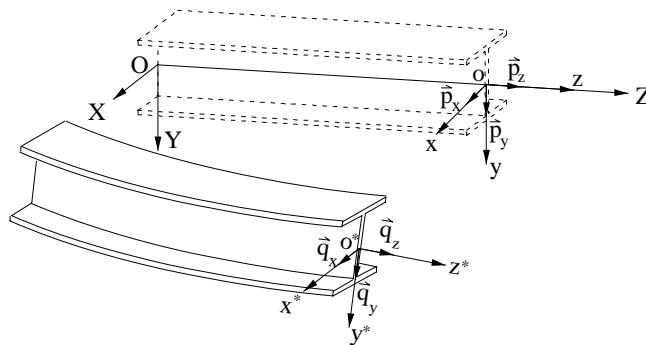


Fig. 1 Deformations of a thin-walled beam

The rotation from vectors  $\vec{p}_x, \vec{p}_y, \vec{p}_z$  to vectors  $\vec{q}_x, \vec{q}_y, \vec{q}_z$  can be described by an orthogonal rotation matrix  $[R]$  as

$$\begin{Bmatrix} \bar{q}_x \\ \bar{q}_y \\ \bar{q}_z \end{Bmatrix} = \begin{bmatrix} R_{11} & R_{12} & R_{13} \\ R_{21} & R_{22} & R_{23} \\ R_{31} & R_{32} & R_{33} \end{bmatrix}^T \begin{Bmatrix} \bar{p}_x \\ \bar{p}_y \\ \bar{p}_z \end{Bmatrix} \quad (1)$$

The components of the rotation matrix are obtained by Pi and Trahair (1994) as

$$\left. \begin{aligned} R_{11} &= \left(1 - \frac{1}{2}u'^2\right)\cos\phi - \frac{1}{2}u'v'\sin\phi, & R_{12} &= -\left(1 - \frac{1}{2}u'^2\right)\sin\phi - \frac{1}{2}u'v'\cos\phi, & R_{13} &= u', \\ R_{21} &= \left(1 - \frac{1}{2}v'^2\right)\sin\phi - \frac{1}{2}u'v'\cos\phi, & R_{22} &= \left(1 - \frac{1}{2}v'^2\right)\cos\phi + \frac{1}{2}u'v'\sin\phi, & R_{23} &= v', \\ R_{31} &= -u'\cos\phi - v'\sin\phi, & R_{32} &= u'\sin\phi - v'\cos\phi, & R_{33} &= 1 + w' \end{aligned} \right\} \quad (2)$$

A second order theory neglects the third and higher order terms and is often used in the buckling and postbuckling analyses because it is considered to have sufficient accuracy. The components of the second order rotation matrix are

$$[R] = \begin{bmatrix} 1 - \frac{1}{2}u'^2 - \frac{1}{2}\phi^2 & -\phi - \frac{1}{2}u'v' & u' \\ \phi - \frac{1}{2}u'v' & 1 - \frac{1}{2}v'^2 - \frac{1}{2}\phi^2 & v' \\ -u' - v'\phi & -v' + u'\phi & 1 - \frac{1}{2}u'^2 - \frac{1}{2}v'^2 \end{bmatrix} \quad (3)$$

A small rotation theory neglects the second and higher order terms and is used for the buckling analysis by a number of researchers because the twist rotation is small during buckling. The components of the small rotation matrix are

$$[R] = \begin{bmatrix} 1 & -\phi & u' \\ \phi & 1 & v' \\ -u' & -v' & 1 \end{bmatrix} \quad (4)$$

## Strains

The longitudinal normal strain of a point  $P(x, y)$  can be obtained as

$$\varepsilon_p = w' + \frac{1}{2}(u'^2 + v'^2) - x(u''C + v''S) + y(u''S - v''C) - \omega\phi'' + \frac{1}{2}(x^2 + y^2)\phi'^2 \quad (5)$$

based on the large rotation matrix (2) where  $C = \cos\phi$  and  $S = \sin\phi$ ,

$$\varepsilon_p = w' + \frac{1}{2}(u'^2 + v'^2) - x(u'' + v''\phi) + y(u''\phi - v'') - \omega\phi'' + \frac{1}{2}(x^2 + y^2)\phi'^2 \quad (6)$$

based on the second order rotation matrix (3), or

$$\varepsilon_p = w' + \frac{1}{2}(u'^2 + v'^2) - x(u'' - v'\phi') - y(u'\phi' + v'') - \omega\phi'' + \frac{1}{2}(x^2 + y^2)\phi'^2 \quad (7)$$

based on the small rotation matrix (4).

The uniform torsion shear strain of a point  $P$  is given by (Vlasov 1961)

$$\gamma_p = -2t_p\phi' \quad (8)$$

where  $t_p$  = the distance of the point  $P$  from the mid-thickness surface.

## Material Plasticity

The onset of yielding is assumed to be governed by the Mises criterion. For a thin-walled member, the Mises yield criterion can be simplified as

$$\sigma_e - \sigma_y = 0 \quad \text{and} \quad \sigma_e = \sqrt{\sigma_p^2 + 3\tau_p^2} \quad (9)$$

where  $\sigma_y$  = uniaxial yield stress,  $\sigma_e$  = effective stress, and  $\sigma_p$  and  $\tau_p$  = the longitudinal normal stress and uniform torsion shear stress, respectively.

Stress increments can be related with strain increments by

$$\{\Delta\sigma_p, \Delta\tau_p\}^T = [E]^{ep} \{\Delta\varepsilon_p, \Delta\gamma_p\}^T \quad (10)$$

where  $[E]^{ep}$  = the elastic-plastic stress-strain matrix given by

$$[E]^{ep} = \begin{bmatrix} E & 0 \\ 0 & G \end{bmatrix} - \frac{1}{\alpha} \begin{bmatrix} \sigma_p^2 E^2 & 3\sigma_p \tau_p EG \\ 3\sigma_p \tau_p EG & 9\tau_p^2 G^2 \end{bmatrix} \quad \text{and} \quad \alpha = \sigma_e^2 H' + \sigma_p^2 E + 9\tau_p^2 G \quad (11)$$

where  $H'$  = strain hardening parameter.

## EFFECTS OF APPROXIMATIONS ON FLEXURAL-TORSIONAL BUCKLING ANALYSIS

### Energy Equation for Flexural-Torsional Buckling

Energy equation for flexural-torsional buckling of a beam can be derived from the second variation of its total potential.

The energy equation based on the second order rotation matrix can be obtained on the basis of strains (6) and (8)

$$\frac{1}{2} \int_0^L \left( EI_y u_b''^2 + GJ \phi_b'^2 + EI_w \phi_b''^2 + 2M_x u_b'' \phi_b' \right) dz = 0 \quad (12)$$

The energy equation based on the small rotation matrix can be obtained on the basis of strains (7) and (8)

$$\frac{1}{2} \int_0^L \left( EI_y u_b''^2 + GJ \phi_b'^2 + EI_w \phi_b''^2 - 2M_x u_b' \phi_b' \right) dz = 0 \quad (13)$$

### Comparison of Energy Equations

The predictions of flexural-torsional buckling moment for a simply supported I-beam subjected to equal and opposite end moments by these two energy equations are the same

$$M = \sqrt{\frac{EI_y \pi^2}{L^2} \left( GJ + \frac{EI_w \pi^2}{L^2} \right)} \quad (14)$$

However, the predictions of the flexural-torsional buckling loads for a simply supported I-beam subjected to a central concentrated load by the energy equation based on the small rotation matrix are substantially higher than those by the energy equation based of the second order rotation matrix as shown in Fig. 2. Also shown in Fig. 2 are test results of Flint (1952), analytical results of Timoshenko and Gere (1961), and ABAQUS (1996) finite element results.

The predictions for a cantilevered I-beam subjected to a tip concentrated load by the energy

equation based on the small rotation matrix are much lower than those by the energy equation based on the second order rotation matrix as shown in Fig. 3. Also shown in Fig. 3 are test results of Anderson and Trahair (1972), analytical results of Timoshenko and Gere (1961), and ABAQUS (1996) finite element results.

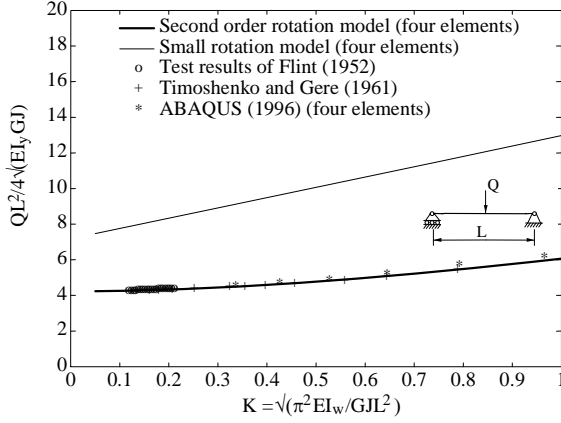


Fig. 2 Lateral buckling of simply supported I-beams

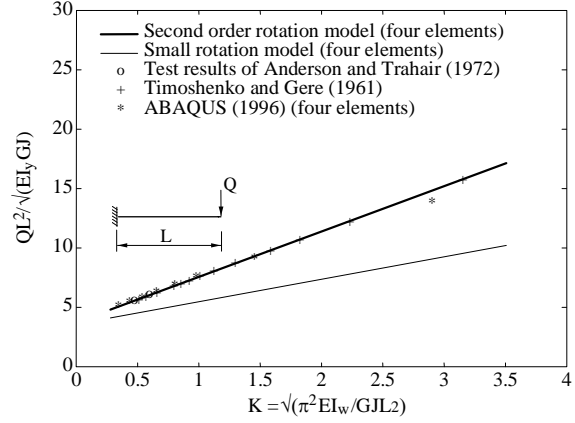


Fig. 3 Lateral buckling of cantilevered I-beams

Predictions by the energy equation based on the second order rotation matrix with four elements agree well with test and analytical results. ABAQUS four element results are less accurate.

This indicates that the energy equation based on the small rotation matrix is not accurate. This has been realised by some researchers who use the small rotation theory in the finite element buckling analysis. They modified the energy equation by adding an additional term  $-\frac{1}{2} \int_0^L 2Qu'_b \phi_b dz$ . The energy equation based on the small rotation matrix is then modified to the same as the energy equation based on the second order rotation matrix because

$$-\frac{1}{2} \int_0^L (2M_x u'_b \phi'_b + 2Qu'_b \phi_b) dz = \frac{1}{2} \int_0^L 2M_x u''_b \phi_b dz \quad (15)$$

when  $M_x$ ,  $u'_b$ , or  $\phi_b$  is equal to zero at both ends of a beam.

It is noted that the shear force in this additional term  $-\frac{1}{2} \int_0^L 2Qu'_b \phi_b dz$  should be calculated from moments  $M_x$  by rigid body equilibrium, not derived from “bending shear strains”. The “shear force” derived from the bending shear strains is not the real one, because bending shear strains should be equal to zero according to Bernoulli assumption. In fact, if a rotation matrix is orthogonal, the bending shear strains obtained from the rotation matrix are equal to zero. Non-zero bending shear strains arise from the fact that the rotation matrix is not orthogonal. Therefore, the additional term is added by the engineering judgment, not by the rigorous mathematical derivation.

## EFFECTS OF APPROXIMATIONS ON POSTBUCKLING ANALYSIS

## Nonlinear Incremental Equilibrium

Nonlinear incremental equilibrium equations can be written as

$$[k]_T \{\Delta r\} = \{\Delta p\} \quad (16)$$

where  $\Delta$  indicates the increment, the load vector is  $\{p\} = \{Q_x, Q_y, Q_z, M_y, M_x, T, B\}^T$ , the node displacement vector is  $\{r\} = \{u_1, v_1, w_1, u'_1, v'_1, \phi_1, u_2, v_2, w_2, u'_2, v'_2, \phi_2\}^T$ , and the tangent stiffness matrix  $[k]_T$  is given by

$$[k]_T = [k] + [k]_G \quad (17)$$

$[k]$  is the displacement stiffness matrix given by

$$[k] = \int_0^L [N]^T [B]^T [D] [B] [N] dz \quad (18)$$

where  $[N]$  = a shape function matrix,  $[B]$  = a matrix describing the relationship of variations of strains of a point with variations of centroid displacements, and  $[D]$  = the tangent modulus matrix given by

$$[D] = \iint [S]^T [E]^{ep} [S] dA \quad (19)$$

where  $[S]$  = the coordinate matrix.

$[k]_G$  is the geometric stiffness matrix given by

$$[k]_G = \int_0^L [N]^T [\Sigma] [N] dz \quad (20)$$

where  $[\Sigma]$  = the stress resultant geometric matrix.

A large rotation model can be developed on the basis of the large rotation matrix (2) and a second order rotation model can be developed on the basis of the second order rotation matrix (3).

## Effects of Approximations

Because the matrix  $[B]$  is related to first variations of strains and the matrix  $[\Sigma]$  is related to second variations of strains, approximations of the second order rotation model may affect the accuracy of matrices  $[B]$  and  $[\Sigma]$ .

For example, contributions of a term  $-xu'' \cos \phi$  of the longitudinal normal strain  $\varepsilon_p$  of (5) to the third row of the matrix  $[B]$  of the large rotation model is

$$[0 \ 0 \ 0 \ 0 \ -\cos \phi \ 0 \ 0 \ u'' \sin \phi \ 0 \ 0] \quad (21)$$

while the contributions of the corresponding term  $-xu''$  of (6) to the second order rotation model is

$$[0 \ 0 \ 0 \ 0 \ -1 \ 0 \ 0 \ 0 \ 0 \ 0] \quad (22)$$

When the twist rotation  $\phi$  is small, contributions of these terms have little difference. However, the difference increases as the twist rotation  $\phi$  increases.

The contributions of the term  $-xu'' \cos \phi$  to the stress resultant geometric matrix  $[\Sigma]$  of the large rotation model are

$$\Sigma(4,8) = \Sigma(8,4) = R_3 \sin \phi \quad \text{and} \quad \Sigma(8,8) = R_3 u'' \cos \phi \quad \text{with} \quad R_3 = \iint x \sigma_p dA \quad (23)$$

while the contribution of the term  $-xu''$  to the second order rotation model is zero.

## Numerical Examples

The first example is flexural-torsional buckling and postbuckling of an elastic aluminium I-section two span continuous beam subjected to concentrated loads  $Q_1$  and  $Q_2$  at mid-span of each span. The self-weight is  $q_y = 77.874$  N/m. Loading, dimensions of the cross-section, and material properties are shown in Fig. 4. To induce flexural-torsional buckling, small initial crookedness ( $u_0 = u_{0c} \sin \pi z / L_1$  and  $u_{0c} = L_1 / 1,000,000$ ) was introduced. The beam was divided into eight equal elements.

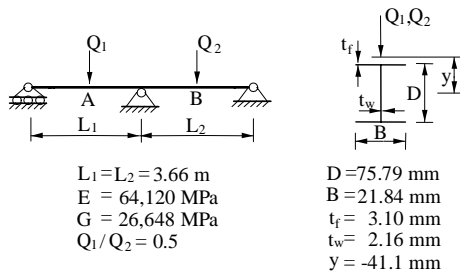


Fig. 4 A continuous beam

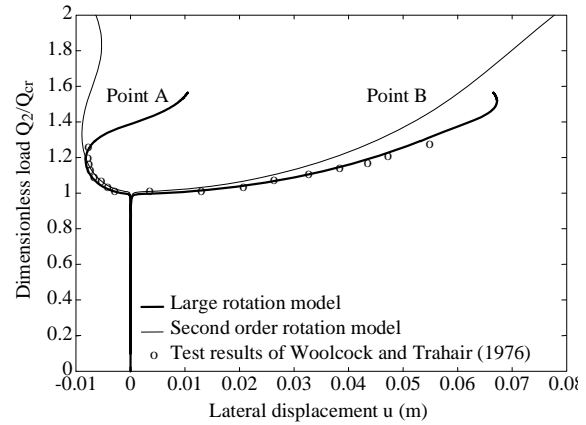


Fig. 5 Buckling and postbuckling of a continuous beam

The results are compared with the test results of Woolcock and Trahair (1972) in Fig. 5 where  $Q_{cr}$  is the value of  $Q_2$  at buckling and  $u$  is the lateral displacements of mid-span A and B. The buckling loads predicted by both the large rotation model and the second order rotation model are the same and agree well with the test results. The postbuckling behaviour predicted by the large rotation model agrees well with the test result. However, the postbuckling behaviour predicted by the second order rotation model is significantly different from the test results.

The second example is torsional buckling and postbuckling of a continuously braced beam. Dimensions of the cross-section and material properties are shown in Fig. 6. The beam is subjected to a central concentrated load  $Q$  at the centre of the top flange ( $y = -130.65$  mm). The beam span is  $L = 4.4$  m. It does not buckle flexural-torsionally because it is laterally continuously braced, but may buckle torsionally. To induce torsional buckling, initial twists of  $\phi_0 = \phi_{0c} \sin \pi z / L$  with  $\phi_{0c} = 0.00088$  radian were introduced. The beam was divided into four equal elements.

Variations of the central twist rotation  $\phi$  with the load  $Q$  are shown in Fig. 7. The elastic buckling load (250.0 kN) predicted by the second order rotation model is higher than that (213.3 kN) predicted by the large rotation model. The inelastic buckling load (134.2 kN) by the second order rotation model is also higher than that (129.6 kN) by the large rotation model. The postbuckling behaviour predicted by the second order rotation model is much stiffer than that predicted by the large rotation model.

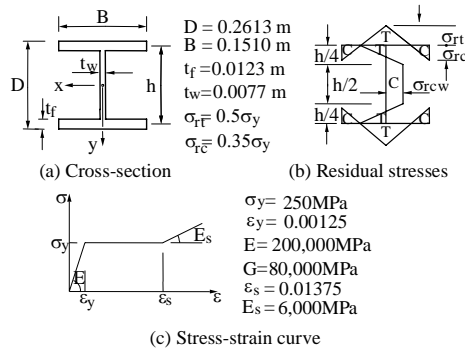


Fig. 6 BHP 10UB29 I-section

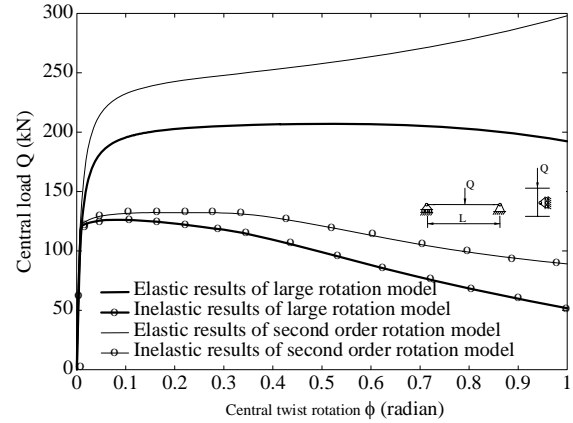


Fig. 7 Torsional buckling and postbuckling of a continuously braced beam

## EFFECTS OF APPROXIMATIONS OF NUMERICAL INTEGRATION

### Numerical Integration Scheme

Numerical integration is usually used to check the yield criterion (9) and to calculate the stress resultants and elastic-plastic stress-strain matrix  $[E]^{ep}$  of (11) after yielding. Numerical integration is approximate and its accuracy is related not only to the integration technique, but also to the arrangement scheme of integration points over the cross-section. Because the effective stress  $\sigma_e$  of (9) consists of longitudinal normal stress  $\sigma_p$  and the uniform torsion shear stress  $\tau_p$ , an integration scheme over the cross-section has to take distributions of both  $\sigma_p$  and  $\tau_p$  into account. Any integration scheme that does not describe the distributions of  $\sigma_p$  or  $\tau_p$  correctly would not perform a correct inelastic analysis. The integration scheme of this paper is compared with the default integration scheme of ABAQUS (1996) beam element in space in Fig. 8. Also shown in Fig. 8 is the uniform torsion shear stress distribution. The shear stress is proportion to the distance from the mid-thickness surface and vanishes at the mid-thickness surface. The ABAQUS integration scheme uses Simpson's three point rule and defines the integration points exactly at the mid-thickness surface where  $\tau_p = 0$ , so that it fails to include any uniform torsion shear stress in the yield criterion. In fact, ABAQUS beam element in space reduces the yield criterion (8) to a uniaxial yield criterion  $\sigma_p = \sigma_y$ . The integration scheme shown in Fig. 8(b) is used in this paper. It consists of eight triangles for each flange and web. Gauss quadrature integration method is used. It is consistent with the distributions of both the longitudinal normal stress and the uniform torsion shear stress, so that the yield criterion, stress resultants and elastic-plastic stress-strain matrix obtained by this scheme are accurate. It can also predict the first yield very well.

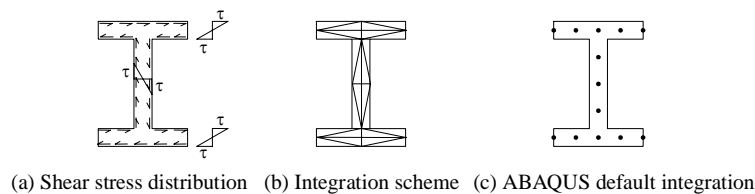


Fig. 8 Integration schemes

### Numerical Example

A simply supported beam subjected to a central concentrated load is used to investigate the



effects of integration schemes. Dimensions of the cross-section and material properties are shown in Fig. 6. The span of the beam is  $L = 4.4$  m. Effects of integration schemes on the inelastic nonlinear postbuckling analysis are demonstrated by comparing elastic load-displacement relationships in Fig. 9 with inelastic load-displacement relationships in Fig. 10. The elastic results of ABAQUS (1996) with eight elements are identical to those of the large rotation model with four elements. The elastic results of ABAQUS with four elements predict a higher buckling load and postbuckling behaviour. The second order rotation model with four elements predicts the correct buckling load but much stiffer postbuckling behaviour. Inelastic results of the second order rotation model are very close to those of the large rotation model except that the postbuckling behaviour is slightly stiffer. ABAQUS inelastic results with four or eight elements predict a higher inelastic buckling load and postbuckling behaviour due to the incorrect integration point scheme over the cross-section.

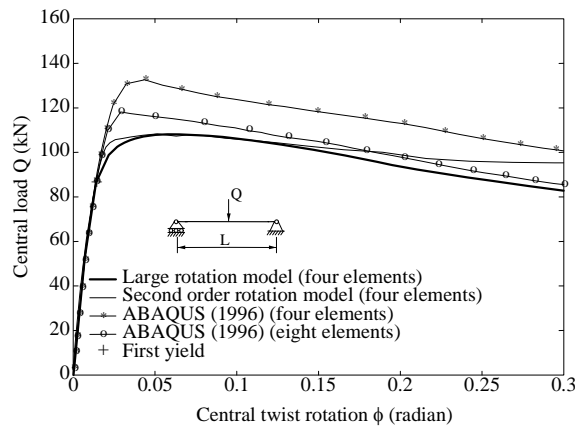
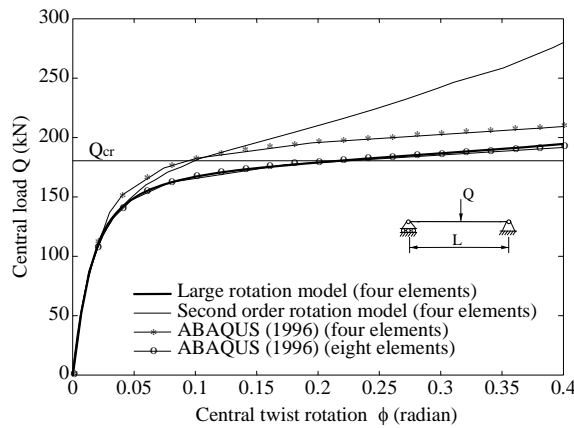


Fig. 9 Elastic buckling and postbuckling

Fig. 10 Inelastic buckling and postbuckling

## CONCLUSIONS

Approximations affect the flexural-torsional buckling and postbuckling analysis of beams significantly in some cases. The energy equation based on the second order rotation matrix predicts correct flexural-torsional buckling loads of beams while the energy equation based on the small rotation matrix does not predict correct bulking loads except for uniform bending. The energy equation based on the small rotation matrix can be modified into the energy equation based on the second order rotation matrix by adding an additional term.

The large rotation model predicts correct elastic and inelastic flexural-torsional buckling and postbuckling behaviour of beams. However, the second order rotation model predicts higher inelastic buckling loads for slender beams and much stiffer postbuckling behaviour because some significant terms are lost in the second order rotation model due to approximations.

The numerical integration scheme over the cross-section needs to be consistent with stress distributions. The default integration scheme over the cross-section of ABAQUS beam element in space is not consistent with stress distributions, so that it does not correctly predict the inelastic flexural-torsional buckling and postbuckling behaviour of beams. The integration scheme over the cross-section proposed in this paper is consistent with the stress distributions and produces correct inelastic flexural-torsional buckling and postbuckling behaviour of beams.

## REFERENCES

- ABAQUS standard user's manual version 5.6* (1996). Hibbit, Karlsson and Sorensen Inc., Abaqus, Pawtucket, R.I., USA.
- Anderson, J.M. and Trahair, N.S. (1972). "Stability of monosymmetric beams and cantilevers." *Journal of Structural Division*, ASCE, 98(1), 269-287.
- Flint, A.R. (1952). "The lateral stability of unrestrained beams." *Engineering*, 170, Dec, 65-67.
- Pi, Y.-L., Trahair, N.S. (1994). "Nonlinear inelastic analysis of steel beam-columns. I: Theory." *Journal of Structural Engineering*, ASCE, 120(7), 2041-2061.
- Simo, J.C. and Vu-Quoc, L. (1987). "The role of non-linear theory in transient dynamic analysis of flexible structures." *Journal of Sound Vibration*, 119(3), 487-508.
- Timoshenko, S.P., and Gere, J.M. (1961). *Theory of elastic stability*. 2nd edition, McGraw-Hill, Inc., New York, N.Y., USA.
- Vlasov, V.Z. (1961). *Thin-walled elastic beams*. 2nd edition, Israel Program for Scientific Translation, Jerusalem, Israel.
- Woolcock, S.T. and Trahair, N.S. (1974). "Post-buckling of redundant I-beams." *Journal of Engineering Mechanics Division*, ASCE, 102(2), 293-312.